Structural Engineering and Mechanics, *Vol. 59, No. 3 (2016) 403-430*
DOI: http://dx.doi.org/10.12989/sem.2016.59.3.403

Dynamics of the oscillating moving load acting on the hydro-elastic system consisting of the elastic plate, compressible viscous fluid and rigid wall

Surkay D. Akbarov*[1,2] and Meftun I. Ismailov[3a]

[1]*Department of Mechanical Engineering, Yildiz Technical University, Yildiz Campus, 34349, Besiktas, Istanbul, Turkey*
[2]*Institute of Mathematics and Mechanics of the National Academy of Sciences of Azerbaijan, 37041, Baku, Azerbaijan*
[3]*Nachicivan State University, Faculty of Mathematics, Nachicivan, Azerbaijan*

(Received December 18, 2015, Revised March 22, 2016, Accepted March 24, 2016)

Abstract. This paper studies the dynamics of the lineal-located time-harmonic moving-with-constant-velocity load which acts on the hydro-elastic system consisting of the elastic plate, compressible viscous fluid - strip and rigid wall. The plane-strain state in the plate is considered and its motion is described by employing the exact equations of elastodynamics but the plane-parallel flow of the fluid is described by the linearized Navier-Stokes equations. It is assumed that the velocity and force vectors of the constituents are continuous on the contact plane between the plate and fluid, and impermeability conditions on the rigid wall are satisfied. Numerical results on the velocity and stress distributions on the interface plane are presented and discussed and the focus is on the influence of the effect caused by the interaction between oscillation and moving of the external load. During these discussions, the corresponding earlier results by the authors are used which were obtained in the cases where, on the system under consideration, only the oscillating or moving load acts. In particular, it is established that the magnitude of the aforementioned interaction depends significantly on the vibration phase of the system.

Keywords: hydro-elastic system; elastic plate; compressible viscous fluid; oscillating moving load; vibration phase

1. Introduction

The modern level of aerospace, nuclear, naval, chemical and biological engineering requires more detailed and exact investigation of plate-fluid interaction problems, the results of which have great significance not only in the theoretical, but also in the application sense. Related investigations were started by Lamb (1921) in which the so-called "non-dimensional added virtual mass incremental" (NAVMI) method was proposed and, by employing this method, vibrations of a circular elastic "baffled" plate in contact with still water were considered. According to the

∗Corresponding author, Professor, E-mail: akbarov@yildiz.edu.tr
[a]Associate Professor, E-mail: imeftun@yahoo.com

http://www.techno-press.org/?journal=sem&subpage=8 ISSN: 1225-4568 (Print), 1598-6217 (Online)

NAVMI method, it is assumed that the contact of the plate with the fluid does not influence its vibration mode and the natural frequency of the plate-fluid system is determined by use of the Rayleigh quotient. It should be noted that according to Lamb (1921), the normal velocity profile of the first mode of vibration of the clamped elastic plate is given through the fourth order polynomial with respect to the radial coordinate. Later, the NAVMI method was also employed in the papers by Kwak and Kim (1991), Kwak (1997), Kwak and Han (2000), Fu and Price (1987), Zhao and Yu (2012) and others listed therein.

Note that up to now, investigations have also been made on the plate-fluid interaction without employing the NAVMI method. An example of such an investigation is the paper by Tubaldi and Armabili (2013) in which the vibration and stability of a rectangular plate immersed in axial liquid flow were studied. Another example is the study carried out in the paper by Charman and Sorokin (2005) in which an asymptotic analysis of sound and vibration when a metal plate radiates sound into water, is given.

An example of another aspect of investigations related to the plate-fluid interaction with regard to wave propagation problems, is the investigation which was made in the paper by Sorokin and Chubinskij (2008) and others listed therein. However, in this paper and all the papers indicated above, the equations of motion of the plate are written within the scope of approximate plate theories by use of the various types of hypotheses such as the Kirchhoff hypothesis for plates. It is evident that in many cases (for instance, in the cases where the wave length is less than the thickness of the plate) the approximate plate theories cannot adequately describe the motion of these plate-fluid systems. Moreover, the foregoing investigations, except the paper by Zhao and Yu (2012), do not take into consideration the initial strains (or stresses) in the plates, which can be one of their characteristics. The use of the exact equations of plate motion and the existence of the initial stresses in the plate are taken into consideration in papers by Bagno (2015), Bagno *et al*. (1994), Bagno and Guz (1997) in which the wave propagation in the pre-stressed plate-compressible viscous fluid systems is studied. Detailed consideration of related results is given in the monograph by Guz (2009).

Employment of the exact three-dimensional field equations on the study of the forced vibration of the hydro-elastic system consisting of the pre-strained highly elastic plate and compressible viscous fluid filling a half - plane, was first made in the paper Akbarov and Ismailov (2014). The forced vibration of the system consisting of the elastic plate, compressible viscous fluid with finite depth and rigid wall was studied in the paper by Akbarov and Ismailov (2015). Moreover, in the paper by Akbarov and Ismailov (2015a), a more detailed review of related investigations is given.

Another aspect of investigations is the dynamic response analysis of plate-fluid systems induced by a moving load. Results of these investigations are applied for construction of floating bridges and for determination of their efficiency. The investigations carried out in the papers by Wu and Shih (1998), Fu *et al*. (2005), Wang *et al*. (2009) and others listed therein can be taken as examples related to the study of the moving load dynamics acting on the plate-fluid systems. However, in these papers the fluid reaction to the plate (i.e., to the floating bridge) is taken into consideration without solution of the equations of the fluid motion. In other words, in these works, the so-called hydrostatic force (denoted by R) caused by the plate-fluid interaction is determined through the linear spring model, i.e., through the reaction $R=-kw$, where w is the vertical displacement of the plate and k is the spring constant. Thus, in the foregoing investigations, the existence of the fluid is taken into consideration only through this spring constant and the approach developed is a very approximate one and cannot answer questions about how the fluid viscosity, fluid depth, fluid compressibility, plate thickness and moving velocity of the external

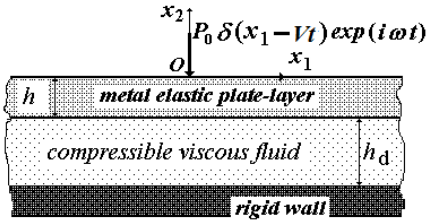

Fig. 1 Sketch of the hydro-elastic system and time-harmonic moving load

force act on the "hydrostatic force" and fluid flow velocities. It is evident that to find the answers to these questions it is necessary to solve the corresponding coupled fluid-plate interaction problems within the scope of the exact linearized equations described for the plate and fluid motions. The first attempt in this field was made in the paper Akbarov and Ismailov (2015b) in which the motion of the plate is described by the exact equations of linear elastodynamics, but the flow of the fluid is described by the linearized Navier-Stokes equations, and the dynamics of the moving load acting on the system consisting of the metal elastic plate, compressible viscous fluid and rigid wall are studied.

Really, any moving load has a certain vibration and therefore such cases can be considered as oscillating moving loads. However, up to now there has not been any investigation related to the study of the dynamics of the oscillating moving load acting on plate-fluid systems. Taking this situation into consideration, in the present paper the first attempt is made in this field and the problem of the dynamics of the time-harmonic oscillating and moving load acting on the system consisting of the elastic plate, compressible viscous fluid and rigid wall, is studied. In other words in the present paper, the investigations carried out in the work by Akbarov and Ismailov (2015a) (in the work by Akbarov and Ismailov (2015b)) are developed for the case where the external force is not only time harmonic (moving), but also moving (time-harmonic).

It should also be noted that the corresponding problems of the dynamics of the oscillating moving load acting on bi-material elastic systems have been studied in the works by Akbarov and Salmanova (2009), Akbarov and Ilhan (2009), Akbarov *et al*. (2015) and a detailed analysis was given in the monograph by Akbarov (2015).

2. Formulation of the problem

Consider a system consisting of the elastic plate-layer, barotropic compressible Newtonian viscous fluid and rigid wall (Fig. 1). We associate the coordinate system $Ox_1x_2x_3$ with the plate and the position of the points of the constituents we determine in this coordinate system. We consider the motion of the plate-layer in the case where the lineal-located time-harmonic force which moves with constant velocity V acts on its free face plane. Assume that the plate occupies the region $\{|x_1|<\infty,\ -h<x_2<0\}$, but the fluid occupies the region $\{|x_1|<\infty,\ -h_d<x_2<-h\}$.

The motion of the plate in the plane strain state in the Ox_1x_2 plane can be described through the following equations of elastodynamics.

$$\frac{\partial \sigma_{11}}{\partial x_1}+\frac{\partial \sigma_{12}}{\partial x_2}=\rho\ \frac{\partial^2 u_1}{\partial t^2},\quad \frac{\partial \sigma_{12}}{\partial x_1}+\frac{\partial \sigma_{22}}{\partial x_2}=\rho\ \frac{\partial^2 u_2}{\partial t^2}.$$

$$\sigma_{11}=(\lambda+2\mu)\varepsilon_{11}+\lambda\varepsilon_{22},\quad \sigma_{22}=\lambda\varepsilon_{11}+(\lambda+2\mu)\varepsilon_{22},\quad \sigma_{12}=2\mu\varepsilon_{12},$$

$$\varepsilon_{11}=\frac{\partial u_1}{\partial x_1},\quad \varepsilon_{22}=\frac{\partial u_2}{\partial x_2},\quad \varepsilon_{12}=\frac{1}{2}\left(\frac{\partial u_1}{\partial x_2}+\frac{\partial u_2}{\partial x_1}\right)\quad . \tag{1}$$

Note that in Eq. (1) conventional notation is used.

Also, consider the equations of motion of the Newtonian compressible viscous fluid: the density, viscosity constants and pressure are denoted by the upper index (1). Thus, according to monograph by Guz (2009), the linearized Navier-Stokes and other field equations for the fluid are

$$\rho_0^{(1)}\frac{\partial v_i}{\partial t}-\mu^{(1)}\frac{\partial v_i}{\partial x_j\partial x_j}+\frac{\partial p^{(1)}}{\partial x_i}-(\lambda^{(1)}+\mu^{(1)})\frac{\partial^2 v_j}{\partial x_j\partial x_i}=0,\quad \frac{\partial\rho^{(1)}}{\partial t}+\rho_0^{(1)}\frac{\partial v_j}{\partial x_j}=0,$$

$$T_{ij}=\left(-p^{(1)}+\lambda^{(1)}\theta\right)\delta_{ij}+2\mu^{(1)}e_{ij},\theta=\frac{\partial v_1}{\partial x_1}+\frac{\partial v_2}{\partial x_2},e_{ij}=\frac{1}{2}\left(\frac{\partial v_i}{\partial x_j}+\frac{\partial v_j}{\partial x_i}\right).a_0^2=\frac{\partial p^{(1)}}{\partial\rho^{(1)}}\quad . \tag{2}$$

where $\rho_0^{(1)}$ is the fluid density before perturbation. The other notation used in Eq. (2) is also conventional.

As presented in the monograph by Guz (2009), the solution of the system of equations in Eq. (2) for 2D plane problems is reduced to finding two potentials φ and ψ which are determined from the following equations

$$\left[\left(1+\frac{\lambda^{(1)}+2\mu^{(1)}}{a_0^2\rho_0^{(1)}}\frac{\partial}{\partial t}\right)\Delta-\frac{1}{a_0^2}\frac{\partial^2}{\partial t^2}\right]\varphi=0,\quad \left(\nu^{(1)}\Delta-\frac{\partial}{\partial t}\right)\psi=0,\quad \Delta=\frac{\partial^2}{\partial x_1^2}+\frac{\partial^2}{\partial x_2^2}, \tag{3}$$

where $\nu^{(1)}$ is the kinematic viscosity, i.e., $\nu^{(1)}=\mu^{(1)}/\rho_0^{(1)}$.

The velocities v_1 and v_2, and the pressure $p^{(1)}$ are expressed by the potentials φ and ψ through the expressions

$$v_1=\frac{\partial\varphi}{\partial x_1}+\frac{\partial\psi}{\partial x_2},\quad v_2=\frac{\partial\varphi}{\partial x_2}-\frac{\partial\psi}{\partial x_1},\quad p^{(1)}=\rho_0^{(1)}\left(\frac{\lambda^{(1)}+2\mu^{(1)}}{\rho_0^{(1)}}\Delta-\frac{\partial}{\partial t}\right)\varphi. \tag{4}$$

Assuming that

$$p^{(1)}=-(T_{11}+T_{22}+T_{33})/3, \tag{5}$$

we obtain

$$\lambda^{(1)}=-\frac{2}{3}\mu^{(1)}\quad . \tag{6}$$

We assume that the following boundary, contact and impermeability conditions are satisfied

$$\sigma_{21}\big|_{x_2=0}=0,\sigma_{22}\big|_{x_2=0}=-P_0\delta(x_1-Vt)e^{i\omega t},\quad \left.\frac{\partial u_1}{\partial t}\right|_{x_2=-h}=v_1\big|_{x_2=-h}\quad ,$$

$$\left.\frac{\partial u_2}{\partial t}\right|_{x_2=-h} = v_2\Big|_{x_2=-h},\ \ \sigma_{21}\big|_{x_2=-h} = T_{21}\Big|_{x_2=-h},\ \ \sigma_{22}\big|_{x_2=-h} = T_{22}\Big|_{x_2=-h},$$

$$v_1\Big|_{x_2=-h-h_d} = 0,\ \ v_2\Big|_{x_2=-h-h_d} = 0, \tag{7}$$

where $\delta(\square)$ is the Dirac delta function.

It should be noted that the present problem differs from that considered in the paper by Akbarov and Ismailov (2014) (in the paper by Akbarov and Ismailov (2015a)). In the paper Akbarov and Ismailov (2014), the boundary condition $\sigma_{22}\big|_{x_2=0} = -P_0\delta(x_1 - Vt)$ (in the paper by Akbarov and Ismailov (2015a), the boundary condition $\sigma_{22}\big|_{x_2=0} = -P_0 e^{i\omega t}$) occurs instead of the boundary condition $\sigma_{22}\big|_{x_2=0} = -P_0\delta(x_1 - Vt)e^{i\omega t}$ in (7) which is used in the present paper.

This completes the formulation of the problem.

3. Method of solution

For the solution of this problem, we use the moving coordinate system $x'_1=x_1-Vt$, $x'_2=x_2$ (below we will omit the upper prime on the new moving coordinates) and first we replace the operators $\partial(\bullet)/\partial t$ and $\partial^2(\bullet)/\partial t^2$ with $(i\omega - V\partial/\partial x_1)$ and $(V^2\partial^2/\partial x_1^2 - 2V\omega i\partial/\partial x_1 - \omega^2)$, respectively. Then substituting the sought functions $g(x_1, x_2, t)$ as $\bar{g}(x_1, x_2)e^{i\omega t}$ (below we will omit the overbar) we obtain the corresponding equations and boundary and contact conditions for the amplitudes of the sought values in the moving coordinate system. For the solution to these equations, we employ the exponential Fourier transformation with respect to the x_1 coordinate

$$f_F(s, x_2) = \int_{-\infty}^{+\infty} f(x_1, x_2)e^{-isx_1}dx_1 \tag{8}$$

to these equations. The originals of the sought values are found through the integrals

$$\frac{1}{2\pi}\int_{-\infty}^{+\infty}\{u_{1F}; u_{2F}; \sigma_{11F}; \sigma_{12F}; \sigma_{22F}; v_{1F}; v_{2F}; T_{11F}; T_{12F}; T_{22F}\}e^{isx_1}ds. \tag{9}$$

Before employing the Fourier transformation (8) we introduce the dimensionless coordinates and dimensionless transformation parameter

$$\bar{x}_1 = x_1/h,\ \ \bar{x}_2 = x_2/h,\ \ \bar{s} = sh. \tag{10}$$

Below we will omit the over-bar on the symbols in (10).

First, we consider the solution of the equations related to the Fourier transformation of the quantities related to the plate-layer, i.e., to the solution of the equations which are obtained from the Eq. (1) after employing the above-noted coordinate and Fourier transformations. Thus, doing some mathematical manipulations we obtain the following equations for u_{1F} and u_{2F}.

$$Au_{1F} - B\frac{du_{2F}}{dx_2} + \frac{d^2u_{1F}}{dx_2^2} = 0 \quad , \quad Du_{2F} + B\frac{du_{1F}}{dx_2} + G\frac{d^2u_{2F}}{dx_2^2} = 0 \, , \tag{11}$$

where

$$A = X^2 - s^2(\lambda/\mu + 2) \quad , \quad B = s(\lambda/\mu + 1) \, ,$$

$$D = X^2 - s^2 \, , \quad G = \lambda/\mu + 2 \quad , X^2 = \omega_1^2 h^2 \Big/ c_2^2 \quad , \quad c_2 = \sqrt{\mu/\rho} \quad . \tag{12}$$

In (12) we use the following notation

$$\omega_1 = \omega - s\frac{V}{h} \tag{13}$$

Introducing the notation

$$A_0 = \frac{AG + B^2 + D}{G} \, , \quad B_0 = \frac{BD}{G} \, , \quad k_1 = \sqrt{-\frac{A_0}{2} + \sqrt{\frac{A_0^2}{4} - B_0}} \quad , \quad k_2 = \sqrt{-\frac{A_0}{2} - \sqrt{\frac{A_0^2}{4} - B_0}} \, , \tag{14}$$

we can write the solution of the Eq. (11) as follows

$$u_{2F} = Z_1 e^{k_1 x_2} + Z_2 e^{-k_1 x_2} + Z_3 e^{k_2 x_2} + Z_4 e^{-k_2 x_2} \quad ,$$

$$u_{1F} = Z_1 a_1 e^{k_1 x_2} + Z_2 a_2 e^{-k_1 x_2} + Z_3 a_3 e^{k_2 x_2} + Z_4 a_4 e^{-k_2 x_2} \, , \tag{15}$$

where

$$a_1 = \frac{-D - Gk_1^2}{Bk_1^2} \quad , \quad a_2 = -a_1 \, , \quad a_3 = \frac{-D - Gk_2^2}{Bk_2^2} \, , \quad a_4 = -a_3 \, . \tag{16}$$

Using the Eqs. (1) and (15) we also write expressions for the Fourier transformations σ_{21F} and σ_{22F} of the corresponding stresses which enter the boundary and contact conditions in (7).

$$\sigma_{21F} = Z_1\left(\omega_{2112}k_1a_1 - s\omega_{2121}\right)e^{k_1x_2} + Z_2\left(-\omega_{2112}k_1a_2 - s\omega_{2121}\right)e^{-k_1x_2} +$$

$$Z_3\left(\omega_{2112}k_2a_3 - s\omega_{2121}\right)e^{k_2x_2} + Z_4\left(-\omega_{2112}k_2a_3 - s\omega_{2121}\right)e^{-k_2x_2} \, ,$$

$$\sigma_{22F} = Z_1\left(s\omega_{2211}a_1 + k_1\omega_{2222}\right)e^{k_1x_2} + Z_2\left(s\omega_{2211}a_2 - k_1\omega_{2222}\right)e^{-k_1x_2} +$$

$$Z_3\left(s\omega_{2211}a_3 + k_2\omega_{2222}\right)e^{k_2x_2} + Z_2\left(s\omega_{2211}a_4 - k_2\omega_{2222}\right)e^{-k_2x_2} \, . \tag{17}$$

This completes consideration of the determination of the Fourier transformation of the values related to the plate-layer. Now we consider determination of the Fourier transformations of the quantities related to the fluid flow. First, we consider the determination of φ_F and ψ_F from the Fourier transformation of the equations in (3). Taking the relation

$$\varphi_F = \omega h^2 \tilde{\varphi}_F \quad , \quad \psi_F = \omega h^2 \tilde{\psi}_F \tag{18}$$

into account, it can be written that

$$\frac{d^2\tilde{\varphi}_F}{dx_2^2}+\left(\frac{\Omega_1^2}{1+i4\Omega_1^2/(3N_w^2)}-s^2\right)\tilde{\varphi}_F=0,\quad \frac{d^2\tilde{\psi}_F}{dx_2^2}-\left(s^2+iN_w^2\right)\tilde{\psi}_F=0, \tag{19}$$

where

$$\Omega_1=\frac{\omega_1 h}{a_0}\quad,\quad N_w^2=\frac{\omega_1 h^2}{\nu^{(1)}}. \tag{20}$$

The dimensionless number N_w in (20) characterizes the influence of the fluid viscosity on the mechanical behavior of the system under consideration. However, the dimensionless frequency Ω_1 in (20) characterizes the influence of the compressibility of the fluid on the mechanical behavior of the system under consideration.

Thus, taking the conditions (6) into consideration, the solutions to the equations in (19) are found as follows

$$\tilde{\varphi}_F=Z_5e^{\delta_1 x_2}+Z_7e^{-\delta_1 x_2}\ ,\ \ \tilde{\psi}_F=Z_6e^{\gamma_1 x_2}+Z_8e^{-\gamma_1 x_2}, \tag{21}$$

where

$$\delta_1=\sqrt{s^2-\frac{\Omega_1^2}{1+i4\Omega_1^2/(3N_w^2)}}\quad,\quad \gamma_1=\sqrt{s^2+iN_w^2}\,. \tag{22}$$

Using (21) and (18) we obtain the following expressions for the velocities, pressure and stresses of the fluid from the Fourier transformations of the Eqs. (2) and (3).

$$v_{1F}=\omega h\left[-Z_5se^{\delta_1 x_2}-Z_7se^{-\delta_1 x_2}+Z_6e^{\gamma_1 x_2}+Z_8e^{-\gamma_1 x_2}\right],$$

$$v_{2F}=\omega h\left[Z_5\delta_1e^{\delta_1 x_2}-Z_7\delta_1e^{-\delta_1 x_2}-Z_6se^{\gamma_1 x_2}-Z_8se^{-\gamma_1 x_2}\right],$$

$$T_{22F}=\mu^{(1)}\omega\left[Z_5\left(\frac{4}{3}\delta_1^2+\frac{2}{3}s^2-R_0\right)e^{\delta_1 x_2}+Z_7\left(\frac{4}{3}\delta_1^2+\frac{2}{3}s^2-R_0\right)e^{-\delta_1 x_2}+\right.$$

$$\left.Z_6\left(-s\gamma_1-\frac{2}{3}s\gamma_1\right)e^{\gamma_1 x_2}+Z_8\left(s\gamma_1+\frac{2}{3}s\gamma_1\right)e^{-\gamma_1 x_2}\right]\ ,$$

$$T_{21F}=-\mu^{(1)}\omega\left[2s\delta_1Z_5e^{\delta_1 x_2}-2s\delta_1Z_7e^{-\delta_1 x_2}+(s^2+\gamma_1^2)Z_6e^{\gamma_1 x_2}+(s^2+\gamma_1^2)Z_8e^{-\gamma_1 x_2}\right],$$

$$p_F^{(1)}=\mu^{(1)}\omega R_0\left(Z_5e^{\delta_1 x_2}+Z_7e^{-\delta_1 x_2}\right), \tag{23}$$

where

$$R_0=-\frac{4}{3}\frac{\Omega_1^2}{1+i4\Omega_1^2/(3N_w^2)}-iN_w^2. \tag{24}$$

Substituting expressions (15), (17) and (23) into the boundary and contact conditions in (7) we obtain a system of equations with respect to the unknowns Z_1, Z_2,…, Z_8 through which the sought

values are determined. These equations can be expressed as follows

$$\left(\sigma_{21F}/\mu\right)\big|_{x_2=0} = Z_1\alpha_{11} + Z_2\alpha_{12} + Z_3\alpha_{13} + Z_4\alpha_{14} = 0\,,$$

$$\left(\sigma_{22F}/\mu\right)\big|_{x_2=0} = Z_1\alpha_{21} + Z_2\alpha_{22} + Z_3\alpha_{23} + Z_4\alpha_{24} = -P_0/\mu\,,$$

$$\left.\frac{\partial u_{1F}}{\partial t}\right|_{x_2=-h} - v_{1F}\big|_{x_2=-h} = i\omega(Z_1\alpha_{31} + Z_2\alpha_{32} + Z_3\alpha_{33} + Z_4\alpha_{34}) -$$

$$\omega h(Z_5\alpha_{35} + Z_6\alpha_{36} + Z_7\alpha_{37} + Z_8\alpha_{38}) = 0\,,$$

$$\left.\frac{\partial u_{2F}}{\partial t}\right|_{x_2=-h} - v_{2F}\big|_{x_2=-h} = i\omega(Z_1\alpha_{41} + Z_2\alpha_{42} + Z_3\alpha_{43} + Z_4\alpha_{44}) -$$

$$\omega h(Z_5\alpha_{45} + Z_6\alpha_{46} + Z_7\alpha_{47} + Z_8\alpha_{48}) = 0\quad,$$

$$\left(\sigma_{21}/\mu\right)\big|_{x_2=-h} - \left(T_{21}/\mu\right)\big|_{x_2=-h} = Z_1\alpha_{51} + Z_2\alpha_{52} + Z_3\alpha_{53} + Z_4\alpha_{54} -$$

$$M(Z_5\alpha_{55} + Z_6\alpha_{56} + Z_7\alpha_{57} + Z_8\alpha_{58}) = 0\quad,$$

$$\left(\sigma_{22}/\mu\right)\big|_{x_2=-h} - \left(T_{22}/\mu\right)\big|_{x_2=-h} = Z_1\alpha_{61} + Z_2\alpha_{62} + Z_3\alpha_{63} + Z_4\alpha_{64} -$$

$$M(Z_5\alpha_{65} + Z_6\alpha_{66} + Z_7\alpha_{67} + Z_8\alpha_{68}) = 0\,,$$

$$v_{1F}\big|_{x_2=-h-h_d} = \omega h(Z_5\alpha_{75} + Z_6\alpha_{76} + Z_7\alpha_{77} + Z_8\alpha_{78}) = 0\,,$$

$$v_{2F}\big|_{x_2=-h-h_d} = \omega h(Z_5\alpha_{85} + Z_6\alpha_{86} + Z_7\alpha_{87} + Z_8\alpha_{88}) = 0\,, \tag{25}$$

where

$$M = \frac{\mu^{(1)}\omega_1}{\mu}\quad. \tag{26}$$

The expressions of the coefficients α_{nm} (n; m=1,2,...8) in (25) can be easily determined from the Eqs. (15), (17) and (23), and therefore they are not given here. Thus, the unknowns Z_1, Z_2,…, Z_8 in the Eq. (25) can be determined via the formula

$$Z_k = \frac{\det\left\|\beta_{nm}^{k}\right\|}{\det\left\|\alpha_{nm}\right\|}\quad. \tag{27}$$

Note that the matrix (β_{nm}^{k}) is obtained from the matrix (α_{nm}) by replacing the k-th column of the latter with the column $(0, -P_0/\mu,0,0,0,0,0,0)^T$.

Now we consider calculation of the integrals in Eq. (9). For this purpose, firstly we consider the following reasoning. If we take the Fourier transformation parameter s as the wavenumber, then the equation

$$\det\left\|\alpha_{nm}\right\| = 0\,,\quad n;m = 1,2,...,8\,, \tag{28}$$

coincides with the dispersion equation of the waves with the velocity ω_1/s propagated in the direction of the Ox_1 axis in the system under consideration. It should be noted that, according to well-known physico-mechanical considerations, the Eq. (28) must have complex roots only for the system under consideration. This character of the roots is caused by the viscosity of the fluid. However, as usual, the viscosity of the Newtonian fluids is insignificant in the qualitative sense and therefore in some cases within the scope of the necessity of the PC calculation accuracy, the Eq. (28) may have "real roots". Consequently, these roots become singular points of the integrated expressions in the integrals (9) and in such cases the algorithm for calculation has been discussed in papers Akbarov and Ilhan (2009), Akbarov *et al*. (2015), Ilhan and Koç (2015), and other works listed in these papers. Moreover, this algorithm was detailed in the monograph by Akbarov (2015), according to which, the wavenumber integrals (9) may be evaluated along the Sommerfeld contour. However, in the present investigation, under calculation of the integrals in (9), the aforementioned "real roots" cases did not arise and, using the representation $g(x_1,x_2,t)=\bar{g}(x_1,x_2)e^{i\omega t}$, the sought values are determined through the following relation

$$\{u_1;u_2;\sigma_{11};\sigma_{12};\sigma_{22};v_1;v_2;T_{11};T_{12};T_{22}\}=\frac{1}{2\pi}\mathrm{Re}\left[e^{i\omega t}\int_{-\infty}^{+\infty}\{u_{1F};u_{2F};\sigma_{11F};\right.$$

$$\left.\sigma_{12F};\sigma_{22F};v_{1F};v_{2F};T_{11F};T_{12F};T_{22F}\}e^{isx_1}ds\right]. \tag{29}$$

During calculation procedures, the improper integral $\int_{-\infty}^{\infty}(\square)ds$ in (29) is replaced by the corresponding definite integral $\int_{-S_1^*}^{S_1^*}(\square)ds$. The values of S_1^* are determined from the convergence requirement of the numerical results. Note that under calculation of the integral $\int_{-S_1^*}^{S_1^*}(\square)ds$, the integration intervals $\left[-S_1^*,+S_1^*\right]$ are further divided into a certain number of shorter intervals which are used in the Gauss integration algorithm. The values of the integrated expressions at the sample points are calculated through the Eq. (25). All these procedures are performed automatically with the PC programs constructed by the authors in MATLAB.

This completes the discussions related to the algorithms employed for calculation of the wave-number integrals in the form (9). Note that after some obvious changes, the foregoing solution method can also be applied for the case where the fluid is inviscid.

4. Numerical results and discussions

According to the foregoing discussions, the problem under consideration is characterized through the dimensionless parameters Ω_1 and N_w which are determined by the expressions in (20); M, which is determined by the expression (26); and λ/μ, where λ and μ are the mechanical constants of the plate material which enter the expression of the elastic relations in Eq. (1). In the numerical investigation, we assume that the material of the plate-layer is Steel with mechanical constants: μ=79×10^9 Pa, λ=94.4×10^9 Pa and density ρ=1160 kg/m^3 (see, Guz and Makhort 2000), but the material of the fluid is Glycerin with viscosity coefficient $\mu^{(1)}$=1,393 kg/(m·s), density ρ=1260 kg/m^3 and sound speed a_0=1927 m/s (see Guz 2009). We also introduce the notation

$c_2=\sqrt{\mu/\rho}$ which is the shear wave propagation velocity in the plate-layer material. After selection of these materials, the foregoing dimensionless parameters can be determined through the following four quantities: h (the thickness of the plate-layer), h_d (the thickness of the fluid strip), V (the load moving velocity) and ω (the frequency of the oscillation of the moving load). Numerical results, which will be discussed below, relate to the normal stress acting on the interface plane between the fluid and plate-layer and to the velocities of the fluid (or of the plate-layer) on the interface plane in the directions of the Ox_1 and Ox_2 axes. We introduce the dimensionless stress $T_{22}h/P_0$ and dimensionless velocities $v_k\mu h/(P_0c_2)$ (k=1,2). To simplify the discussion below, we also denote the following three cases.

$$\text{Case 1: } V=0 \text{ and } \omega\neq 0\text{; Case 2: } V\neq 0 \text{ and } \omega=0\text{;}$$
$$\text{and Case 3: } V\neq 0 \text{ and } \omega\neq 0\,. \tag{30}$$

As follows from the physico-mechanical considerations and from the investigations carried out in the paper by Akbarov and Ismailov (2015a), in Case 1 the distribution of the stress $T_{22}h/P_0$ and the velocity $v_2\mu h/(P_0c_2)$ (the velocity $v_1\mu h/(P_0c_2)$) are symmetric (are asymmetric) with respect to the point x_1/h=0. However, in Case 2, as noted in the paper by Akbarov and Ismailov (2015b), as a result of the fluid viscosity, the aforementioned symmetry and asymmetry are violated. As will be shown below and as follows from the physico-mechanical considerations, the above-noted symmetry and asymmetry are also violated in Case 3. How the magnitude of this violation depends on the vibration phase ωt and on the dimensionless fluid depth h_d/h is the main subject of the present numerical investigations. Throughout these investigations, we assume that h=0.01 m and x_2/h=−1.

We begin the discussions of the numerical results with consideration of the convergence of the calculation algorithm.

4.1 Convergence of the numerical results

As noted above, under calculation of the integrals in (29) the values of S_1^* are determined from the convergence criterion of these integrals. The results obtained for various problem parameters show that the very disadvantaged case, in the convergence sense, appears for low vibration frequency and low moving velocity and for the small values of the ratio h_d/h. Therefore, for illustration of this convergence, we assume that ω=50 hz, V/h=100 hz and h_d/h=2, and consider the case where ωt=0.

Under calculation of these integrals, the interval $[-S_1^*,+S_1^*]$ is divided into a certain number of shorter intervals. Let us denote this number through $2N$. Consequently, the length of these shorter intervals is S_1^*/N and in each of these shorter intervals the integration is made by the use of the Gauss integration algorithm with ten sample points. Consequently, convergence of the numerical integration can be estimated with respect to the values of S_1^* and N.

Thus, we consider examples of the convergence of the numerical results with respect to the number N in the case where $S_1^*=5$. Analyze the graphs given in Fig. 2 which illustrate the distribution of the dimensionless stress $T_{22}h/P_0$ (Fig. 2(a)) and dimensionless velocities $v_2\mu h/(P_0c_2)$ (Fig. 2(b)) and $v_1\mu h/(P_0c_2)$ (Fig. 2(c)) with respect to x_1/h for various values of the number N. It follows from the analyses of the results given in Fig. 2 that in the cases where $N\geq$50 the results obtained for various values of N coincide with each other with accuracy 10^{-6}–10^{-7}. Nevertheless,

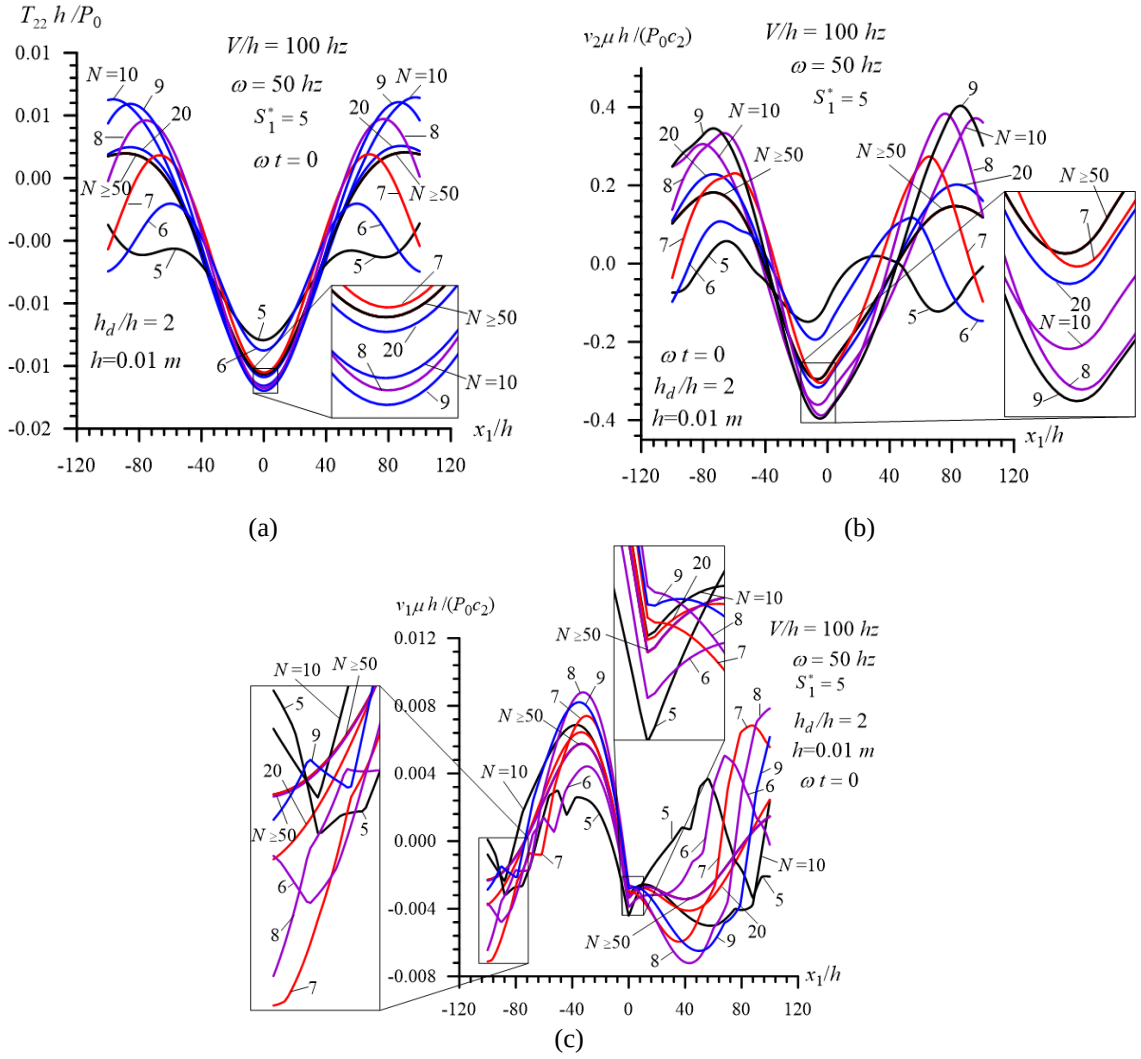

Fig. 2 Convergence of the results related to the stress $T_{22}h/P_0$ (a), and velocities $v_2\mu h/(P_0c_2)$ (b) and $v_1\mu h/(P_0c_2)$ (c) with respect to the number N

under obtaining all the numerical results which will be discussed below, it is assumed that N=300.

Consider also the graphs which illustrate the convergence of the numerical results with respect to the integrating interval, i.e., with respect to the values of S_1^*. These graphs are given in Fig. 3(a) for the dimensionless stress $T_{22}h/P_0$, and in Figs. 3(b) and 3(c) for the dimensionless velocities $v_2\mu h/(P_0c_2)$ and $v_1\mu h/(P_0c_2)$, respectively. Under construction of these graphs it is assumed that $N = 300$. It follows from these graphs that the numerical results approach a certain asymptote with S_1^*, and, with x_1/h, the convergence of the numerical results with respect to S_1^* requires an increase in the values of S_1^*. In obtaining the numerical results, which will be discussed below, all the foregoing particularities relating to the convergence of the numerical results are taken into consideration and it is established that the case where $S_1^* = 5$ is quite sufficient for obtaining

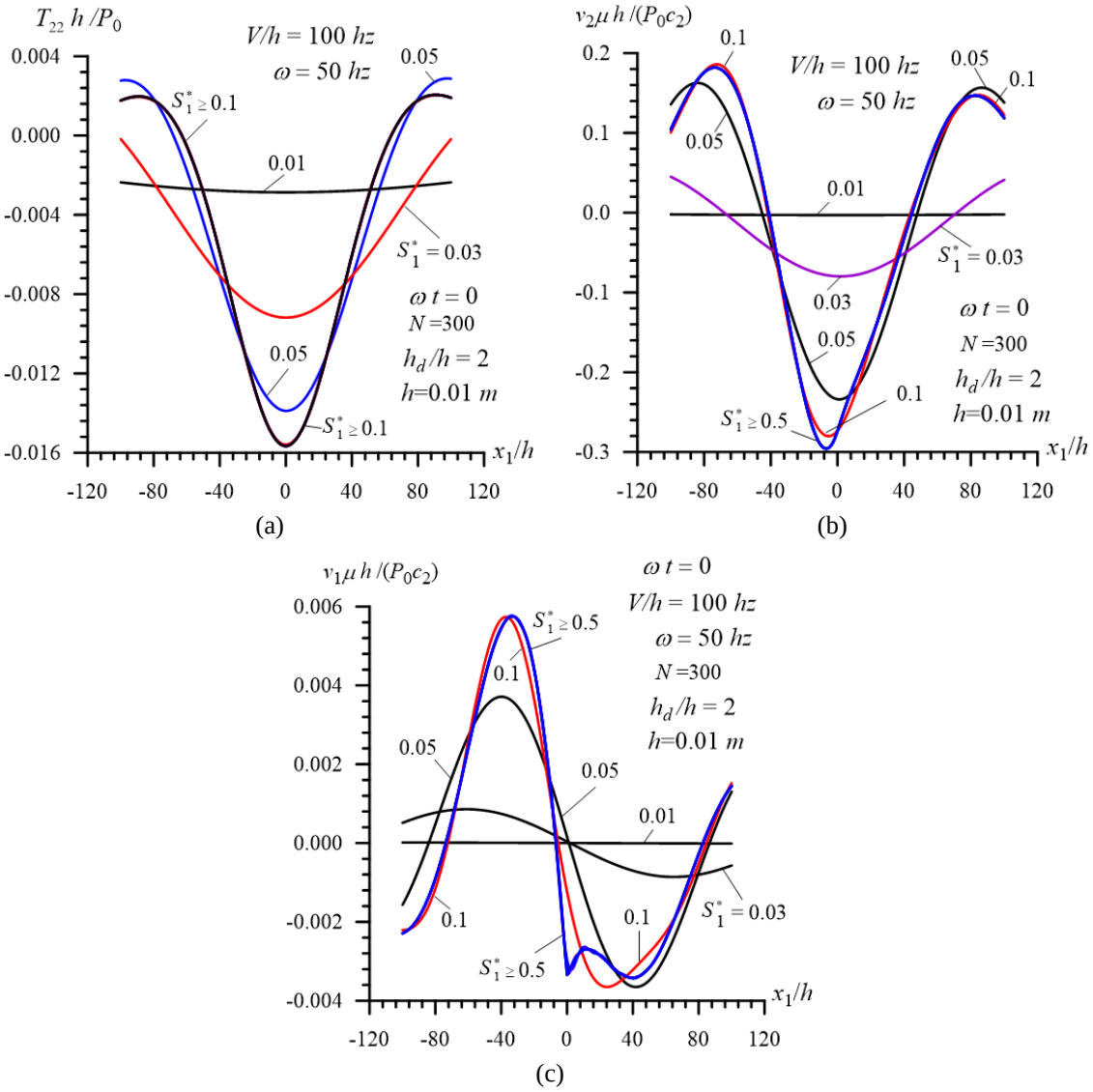

Fig. 3 Convergence of the results related to the stress $T_{22}h/P_0$ (a), and velocities $v_2\mu h/(P_0c_2)$ (b) and $v_1\mu h/(P_0c_2)$ (c) with respect to the integration interval $[-S_1^*,+S_1^*]$

verified results. At the same time, it should be noted that the foregoing convergence results can also be taken as validation of the algorithm and programs used. Unfortunately, we have not found any related results of other authors in order to compare with the present ones. Therefore validation of the present results can be proven with the convergence of the numerical results, with the consistency of the results with mechanical considerations and with the fact that the results obtained in the present paper which are related to Case 1 and Case 2 coincide with the corresponding ones obtained in the papers by Akbarov and Ismailov (2015a), Akbarov and Ismailov (2015b), respectively.

4.2 The influence of the moving of the oscillating load on the stress and velocities' distributions

First we recall some results obtained in Case 1 and Case 2 indicated in (30), i.e., obtained in the papers by Akbarov and Ismailov (2015a), Akbarov and Ismailov (2015b), respectively. Thus, according to the paper by Akbarov and Ismailov (2015a), in Case 1 the stress $T_{22}h/P_0$ and velocity $v_2\mu h/(P_0c_2)$ have their absolute maximum values at the point $x_1/h=0$, however, the velocity $v_1\mu h/(P_0c_2)$ has its maximum at the point $x_1/h=(x_1/h)^*>0$ and the values of $(x_1/h)^*$ depend on the problem parameters. Moreover, in the paper Akbarov and Ismailov (2015a) it was established that the stress $T_{22}h/P_0$ has its absolute maximum (the velocities $v_2\mu h/(P_0c_2)$ and $v_1\mu h/(P_0c_2)$ have their zeroth) with respect to the vibration phase ωt in the cases where $\omega t=(\omega t)^*+n\pi$ and the values of $(\omega t)^*$ are near to zero, but the velocities $v_2\mu h/(P_0c_2)$ and $v_1\mu h/(P_0c_2)$ have their absolute maximum (the stress $T_{22}h/P_0$ has its zeroth) with respect to the vibration phase ωt in the cases where $\omega t=(\omega t)^{**}+n\pi$ and the values of $(\omega t)^{**}$ are near to $\pi/2$. Taking these statements into consideration, below we will examine the influence of the simultaneous vibration and moving of the external load on the stress and velocities' distributions in the cases where $\omega t=0$ and $\omega t=\pi/2$.

Thus, taking the foregoing discussions into account, we consider the distribution of the stress $T_{22}h/P_0$ and velocities $v_2\mu h/(P_0c_2)$ and $v_1\mu h/(P_0c_2)$ with respect to x_1/h, the graphs of which are given in Figs. 4(a), 4(b) and 4(c), respectively. Note that these graphs are constructed for various values of the ratio h_d/h in the case where ω=50 hz. Moreover, note that under construction of the graphs related to the stress $T_{22}h/P_0$ (Fig. 4(a)) it is assumed that $\omega t=0$, and under construction of the graphs related to the velocities $v_2\mu h/(P_0c_2)$ (Fig. 4(b)) and $v_1\mu h/(P_0c_2)$ (Fig. 4(c)) it is assumed that $\omega t=\pi/2$.

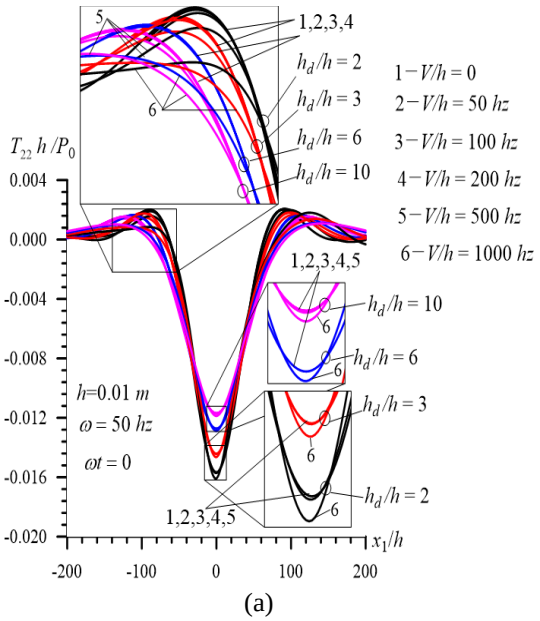

(a)

Fig. 4 The influence of the moving velocity V/h of the oscillation load and of the fluid depth h_d/h on the distribution of the stress $T_{22}h/P_0$ (a) under $\omega t=0$, and velocities $v_2\mu h/(P_0c_2)$ (b) and $v_1\mu h/(P_0c_2)$ (c) under $\omega t=\pi/2$

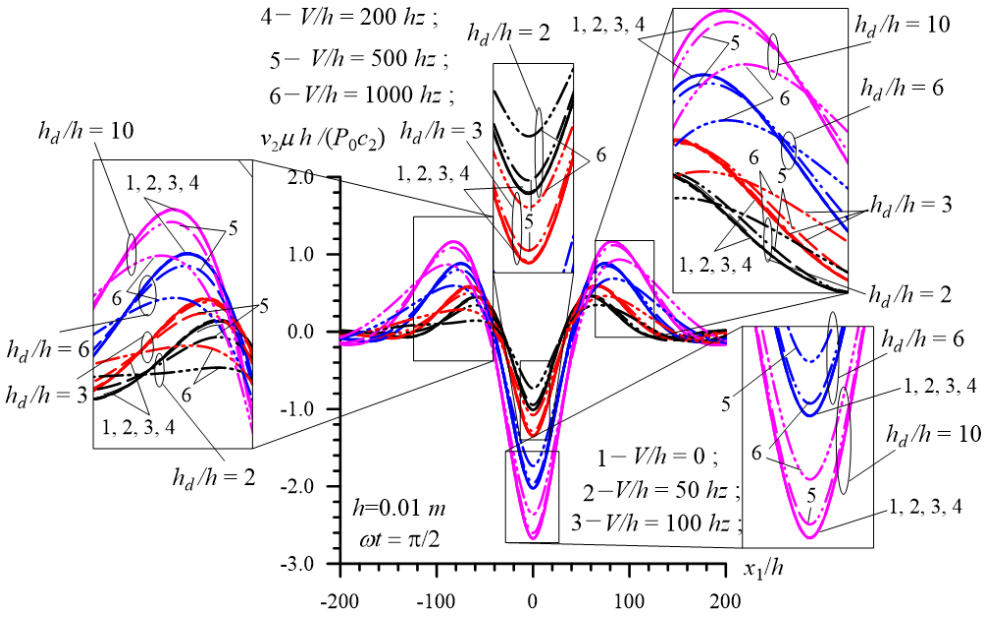

(b)

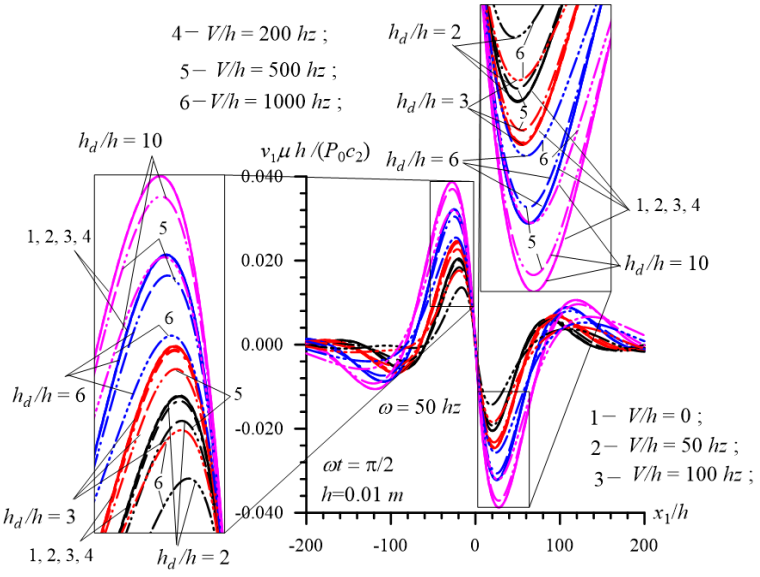

(c)

Fig. 4 Continued

Now we consider the numerical results illustrating how the interaction between the moving and oscillation of the external load acts on the distributions under consideration. Consider the graphs given in Figs. 5-10 each of which simultaneously illustrate the studied distributions obtained in Case 1, Case 2 and Case 3 (30) for various values of the ratio h_d/h. Note that the results given in Figs. 5 and 6 relate to the stress $T_{22}h/P_0$, however, the results given in Figs. 7 and 8 (in Figs. 9 and 10) relate to the velocity $v_2\mu h/(P_0c_2)$ (to the velocity $v_1\mu h/(P_0c_2)$). Moreover note that the graphs

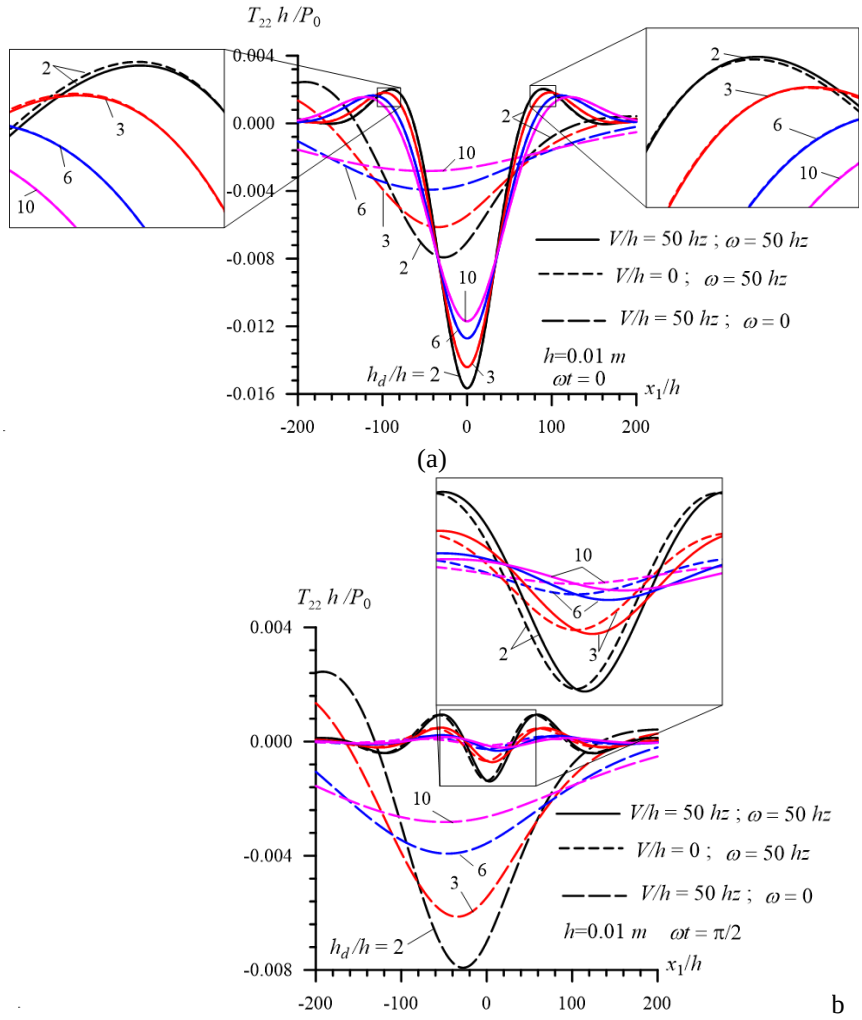

Fig. 5 Distribution of the stress $T_{22}h/P_0$ in Case 1, in Case 2 and in Case 3 (30) under ω=50 hz in the cases where ωt=0 (a) and ωt=π/2 (b)

grouped by the letter a (by the letter b) are constructed in the case where ωt=0 (in the case where ωt=π/2). Under construction of the graphs given in Figs. 5, 7 and 9 (in Figs. 6, 8 and 10) it is assumed V/h=0 and ω=50 hz in Case 1; V/h=50 hz and ω=0 in Case 2; and V/h=50 hz and ω=50 hz in Case 3 (V/h=0 and ω=100 hz in Case 1; V/h=100 hz and ω=0 in Case 2; and V/h=100 hz and ω=100 hz in Case 3), respectively.

Thus, we analyze the foregoing results and begin with the Figs. 5 and 6, according to which, it can be concluded that the difference between the results obtained in Case 2 and in Case 3 is more significant than that obtained in Case 1 and in Case 3. In the case where ωt=0 (in the case where ωt=π/2) the absolute maximum values of the stress obtained in Case 1 and in Case 3 (in Case 2) are significantly greater than those obtained in Case 2 (in Case 1 and in Case 3). It also follows from the Figs. 5 and 6 that in Case 2 and in Case 3, the symmetry of the distribution of the stress $T_{22}h/P_0$ with respect to x_1/h=0 is violated and this violation becomes more significant with

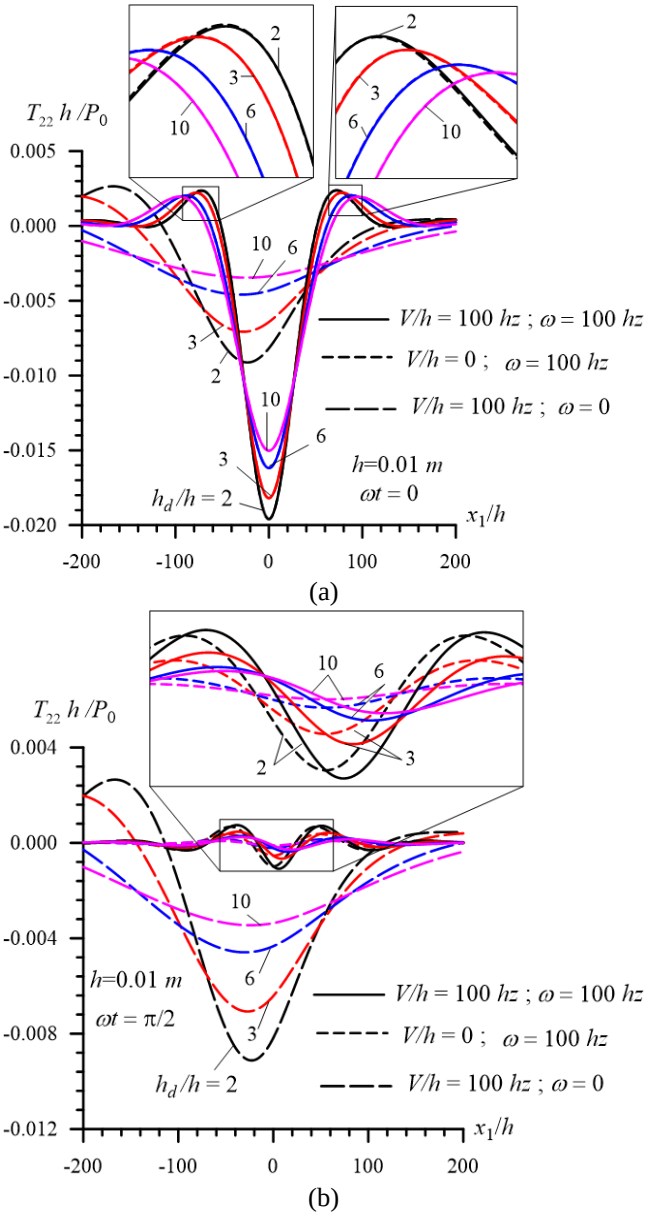

Fig. 6 Distribution indicated in Fig. 5 and obtained under ω=100 hz

decreasing of the ratio h_d/h, i.e., with decreasing of the fluid depth. Observation of the graphs show that the magnitude of this violation in Case 2 is significantly greater than in Case 3. At the same time, the violation is insignificant (is considerable) in Case 3 under ωt=0 (under ωt=π/2 Consequently, according to the foregoing results, it can be concluded that the influence of the moving of the oscillation load on the stress distribution caused with this load in the case where ωt=π/2 is more significant than in the case where ωt=0.

The analyses of the results given in Figs. 7 and 8 show that the foregoing discussion made for

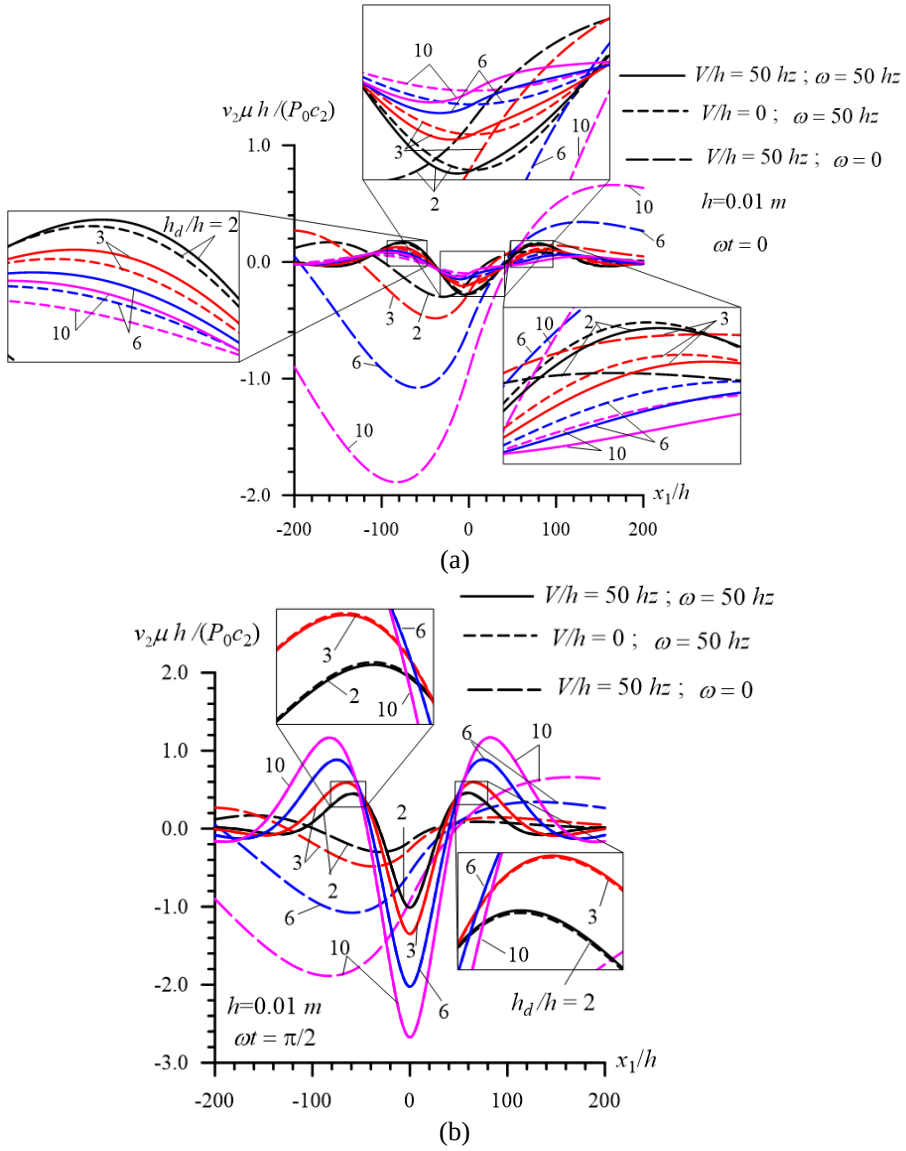

Fig. 7 Distribution of the stress $v_2\mu h/(P_0c_2)$ in Case 1, in Case 2 and in Case 3 (30) under ω=50 hz in the cases where ωt=0 (a) and ωt=π/2 (b)

the stress $T_{22}h/P_0$ can be repeated in the qualitative sense for the velocity $v_2\mu h/(P_0c_2)$. However, under this discussion ωt=0 must be replaced with ωt=π/2 and vise-versa. The results obtained for the stress $T_{22}h/P_0$ under ωt=0 (under ωt=π/2) are also obtained in the qualitative sense for the velocity $v_2\mu h/(P_0c_2)$ under ωt=π/2 (under ωt=0). Consequently, according to the results given in Figs. 7 and 8, it can be concluded that the influence of the moving of the oscillation load on the distribution of the velocity $v_2\mu h/(P_0c_2)$ caused with this load, in the case where ωt=0 is more significant than in the case where ωt=π/2.

Now we consider the distribution related to the velocity $v_1\mu h/(P_0c_2)$ and given in Figs. 9 and 10.

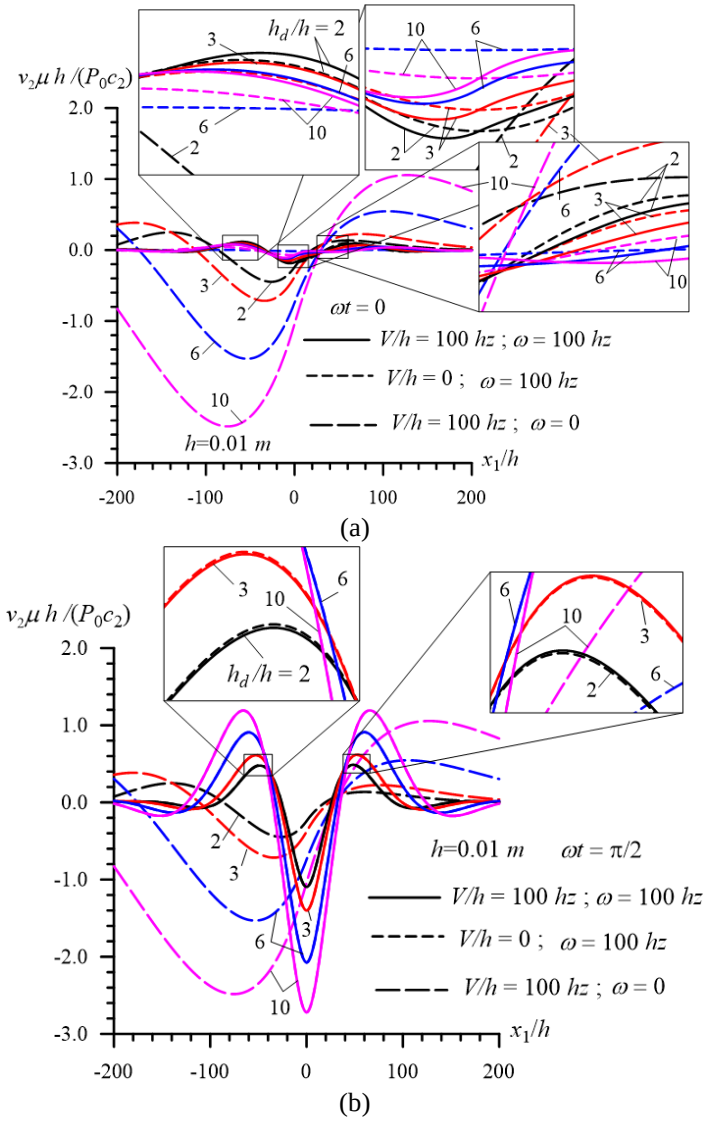

Fig. 8 Distribution indicated in Fig. 7 and obtained under ω=100 hz

We recall that this distribution is asymmetric in Case 1 and as follows from the Figs. 9 and 10 this asymmetry is violated in Case 2 and in Case 3. The magnitude of the violation in Case 2 is significant, however, in Case 3 the magnitude of the violation depends on the vibration phase. For instance, in the case where ωt=0, the magnitude of the asymmetry violation in Case 3 becomes more significant and considerable than in the case where $\omega t=\pi/2$. Moreover, the results illustrated in Figs. 9 and 10 show that under $\omega t=\pi/2$ (under ωt=0) the absolute values of the velocity $v_1\mu h/(P_0c_2)$ obtained in Case 1 and in Case 3 (in Case 2) are significantly greater than those obtained in Case 2 (in Case 1 and in Case 3). Consequently, the results show that the influence of the moving of the oscillation load on the distribution of the velocity $v_1\mu h/(P_0c_2)$ caused with this load, as well as on the distribution of the velocity $v_2\mu h/(P_0c_2)$, in the case where ωt=0, is more

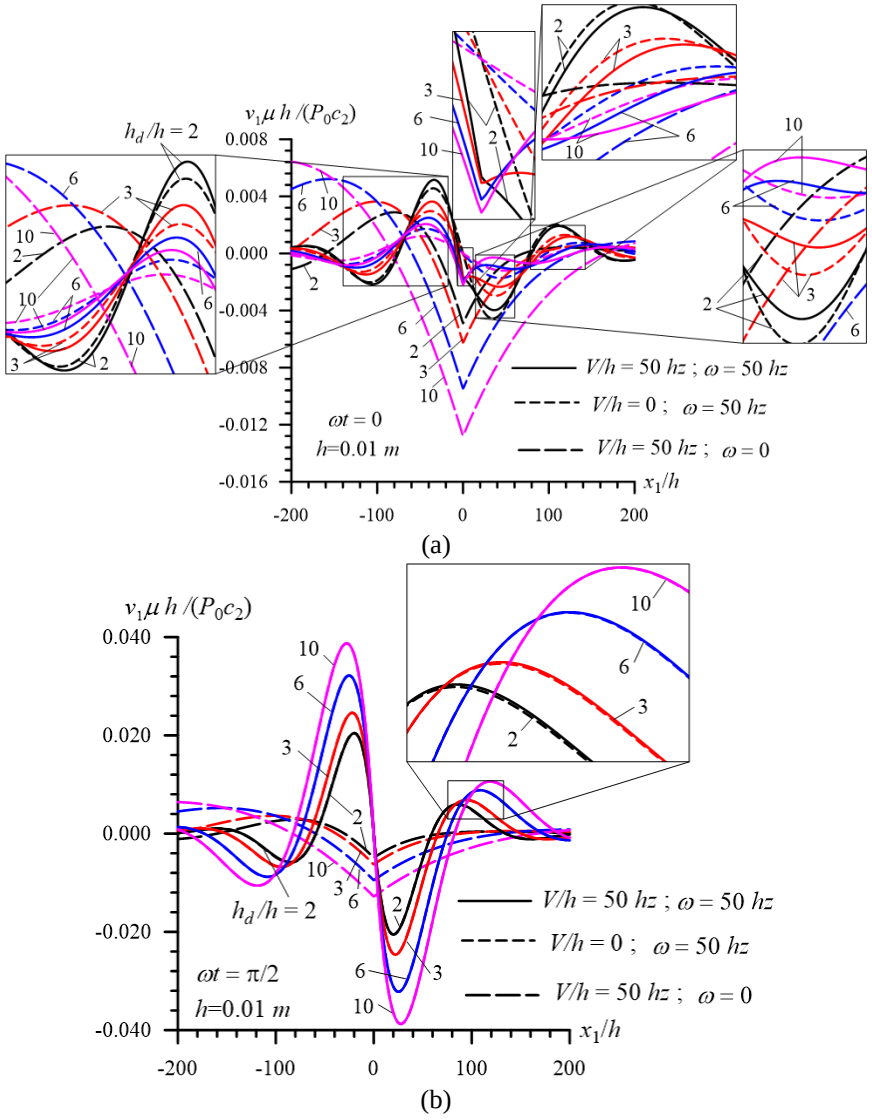

Fig. 9 Distribution of the stress $v_1\mu h/(P_0c_2)$ in Case 1, in Case 2 and in Case 3 (30) under ω=50 hz in the cases where ωt=0 (a) and ωt=π/2 (b)

significant than in the case where ωt=π/2.

Thus, we can conclude that the influence of the moving of the oscillating load on the stress distribution (on the velocities' distributions) caused with this load becomes considerable in the case where ωt=π/2 (in the case where ωt=0). More precisely, the foregoing conclusion can be formulated as follows: the influence of the moving of the oscillating load on the stress distribution (on the velocities' distributions) caused with this load becomes considerable in the case where ωt=(ωt)**+$n\pi$ (in the case where ωt=(ωt)*+$n\pi$).

Taking the foregoing conclusion into consideration, now we consider the results which illustrate how an increase in the values of the moving velocity of the oscillating load acts on the

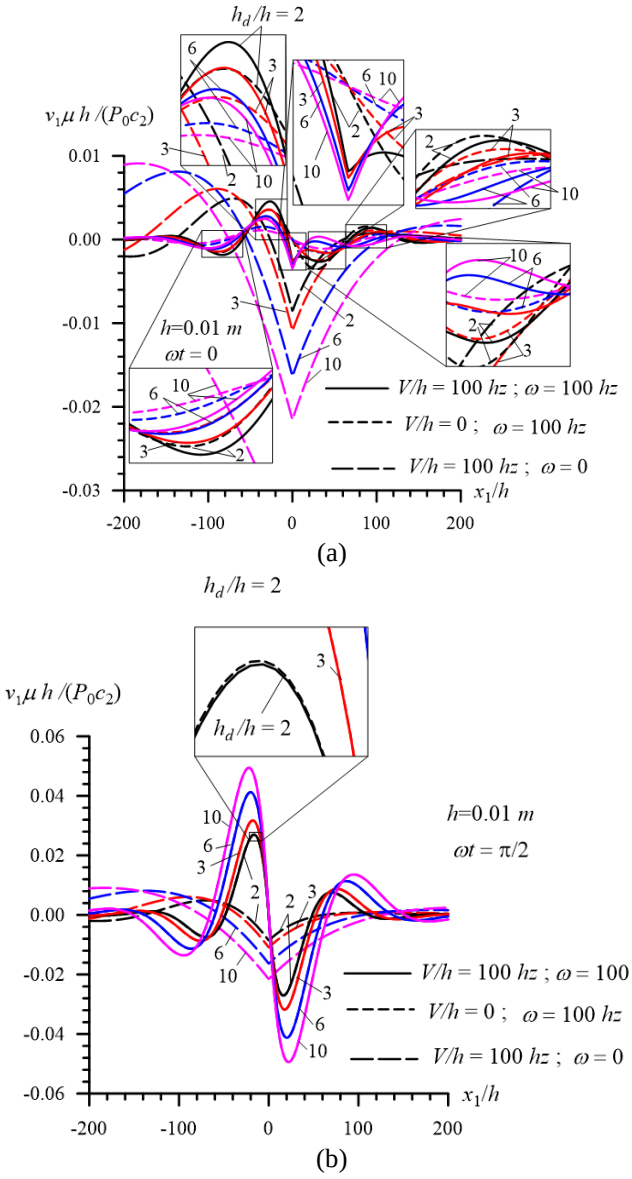

Fig. 10 Distribution indicated in Fig. 9 and obtained under ω=100 hz

stress distribution (on the velocities' distribution) in the case where $\omega t=\pi/2$ (in the case where ωt=0). These results, obtained for the stress $T_{22}h/P_0$, and velocities $v_2\mu h/(P_0c_2)$ and $v_1\mu h/(P_0c_2)$ for various values of the moving velocity V/h in the case where ω=50 hz, are given in Figs. 11, 12 and 13, respectively. In these figures, the graphs grouped by the letters *a*, *b* and *c* correspond to the cases where h_d/h=2, 6 and 10, respectively.

It follows from these results that an increase in the moving velocity of the oscillation load changes, significantly, the distributions under consideration, not only in the quantitative sense, but also in the qualitative sense. For instance, the symmetric (asymmetric) distribution of the stress

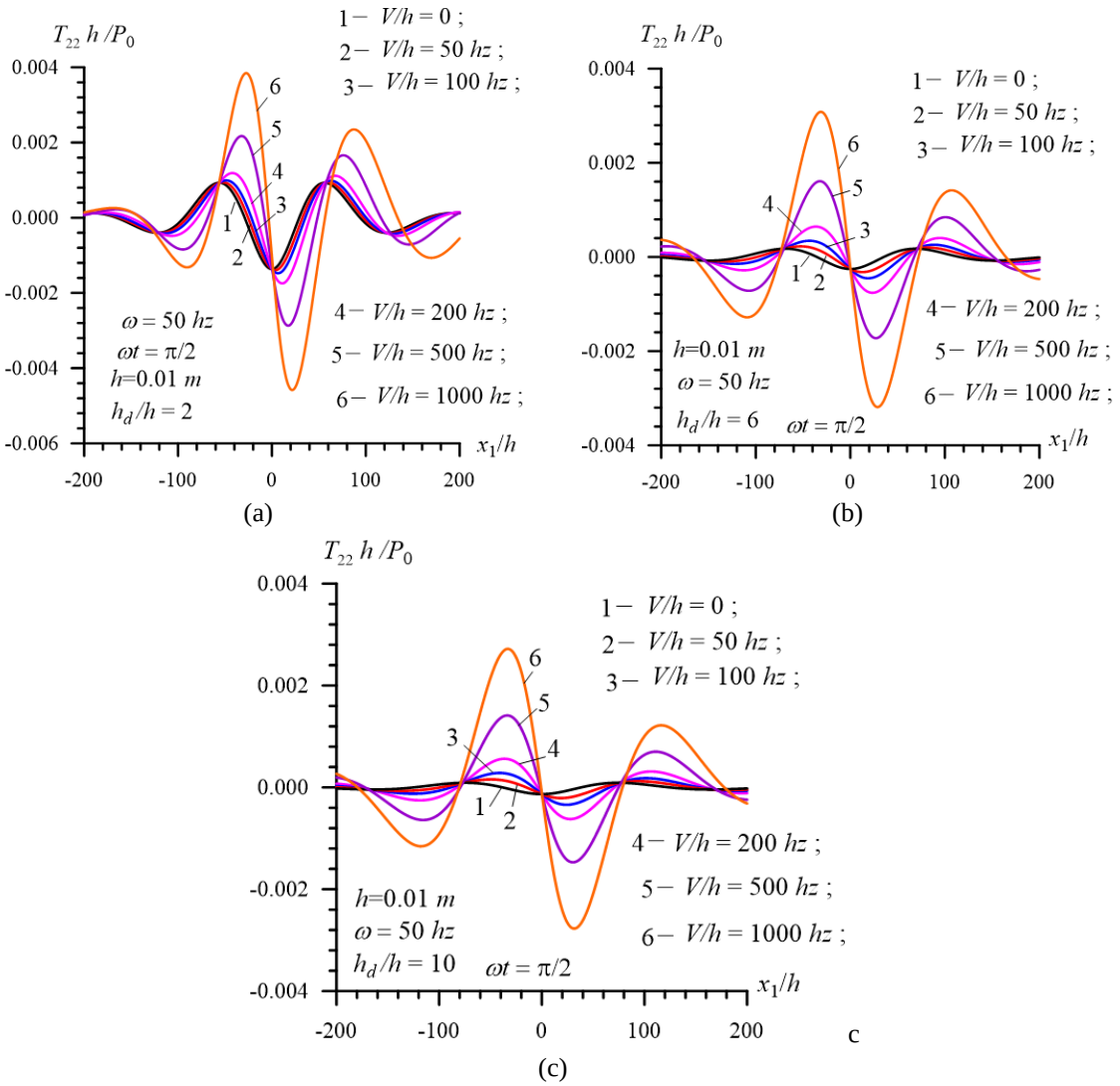

Fig. 11 The influence of the moving velocity of the oscillation load on the distribution of the stress $T_{22}h/P_0$ under $\omega t=\pi/2$ in the cases where h_d/h=2 (a), 6 (b) and 10 (c)

$T_{22}h/P_0$ and velocity $v_2\mu h/(P_0c_2)$ (of the velocity $v_1\mu h/(P_0c_2)$) with respect to x_1/h=0 obtained in the case where V/h=0 becomes quasi-asymmetric (quasi-symmetric) with moving velocity V/h. Comparison of the results given through the graphs grouped by the letters *a*, *b* and *c* with each other show that the absolute maximum values of the stress $T_{22}h/P_0$ (of the velocities $v_2\mu h/(P_0c_2)$ and $v_1\mu h/(P_0c_2)$ decrease (increase) with the fluid depth, i.e., with the ratio *hd/h*.

For estimation of the influence of the fluid viscosity on the considered distributions here we also consider some of the results obtained in the case where the fluid (in this case, the Glycerin) is modelled as inviscid. We consider the distribution of the stress $T_{22}h/P_0$ and the velocity $v_2\mu h/(P_0c_2)$ only, because, as noted in the papers by Akbarov and Ismailov (2015a) and Akbarov and Ismailov (2015b), the values of the velocity $v_1\mu h/(P_0c_2)$ obtained for the inviscid fluid case are not

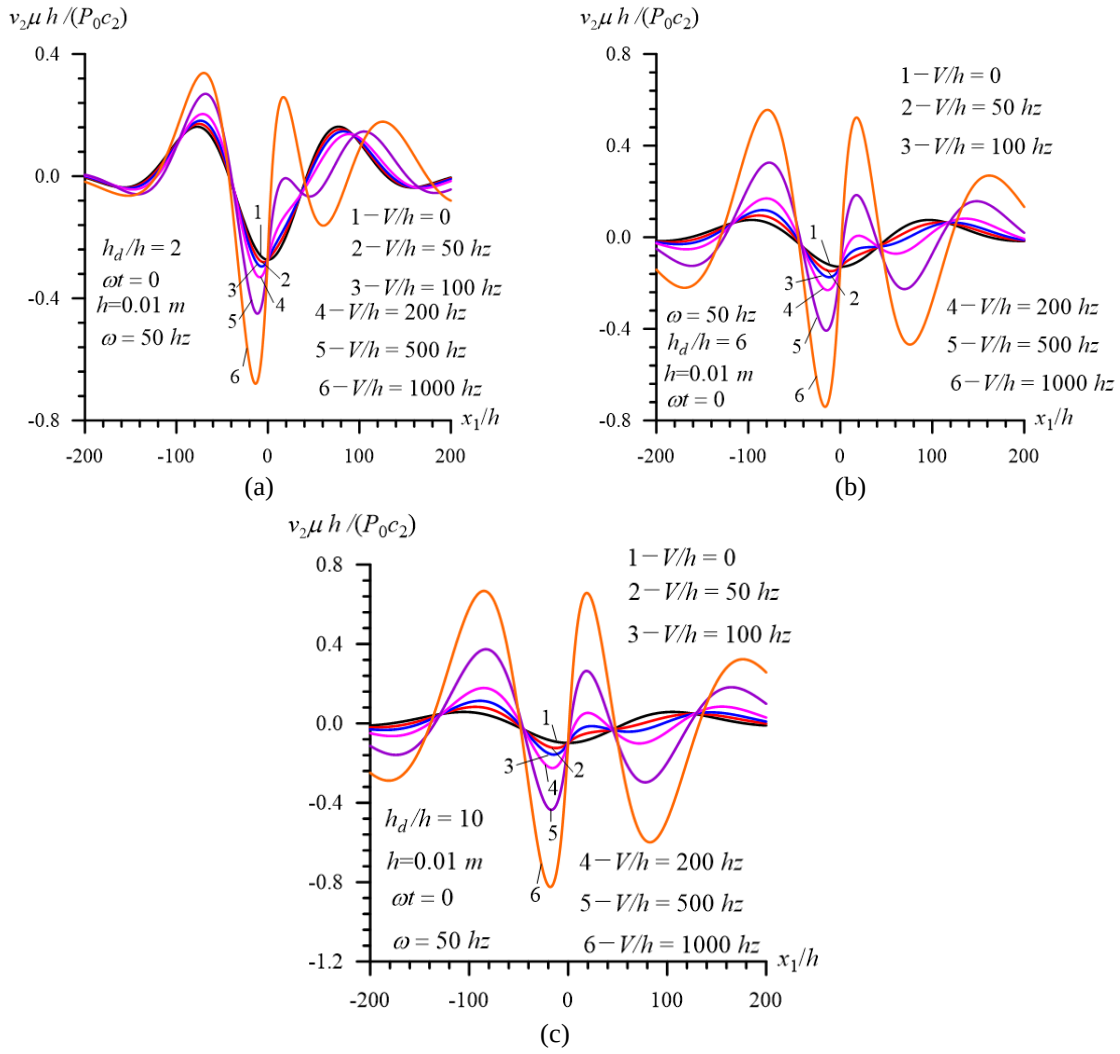

Fig. 12 The influence of the moving velocity of the oscillation load on the distribution of the velocity $v_2\mu h/(P_0c_2)$ under ωt=0 in the cases where h_d/h=2 (a), 6 (b) and 10 (c)

comparable with those obtained in the viscous fluid case.

Thus, consider the graphs given in Figs. 14 and 15 which illustrate the distribution of the stress $T_{22}h/P_0$ and the velocity $v_2\mu h/(P_0c_2)$, respectively in the case where h_d/h=2 and ω=50 hz. In these figures, the graphs grouped by the letters *a* and *b* are constructed in the cases where ωt=0 and ωt=π/2, respectively. According to the paper by Akbarov and Ismailov (2015), we recall that under V/h=0 in the inviscid fluid case, the value of $(\omega t)^*$ (at which the stress has its absolute maximum) is equal to zero, however, the value of $(\omega t)^{**}$ (at which the velocities have their absolute maxima) is equal to π/2. Moreover, we also recall that in the case where $\omega t=\pi/2+n\pi$ (in the case where $\omega t=0+n\pi$) the values of the stress (the values of the velocities) are equal to zero.

It follows from the results given in Fig. 14(a) (in Fig. 15(b)) and from comparison of these results with the corresponding ones given in Fig. 4(a) (in Fig. 4(b)) that the effect of the fluid

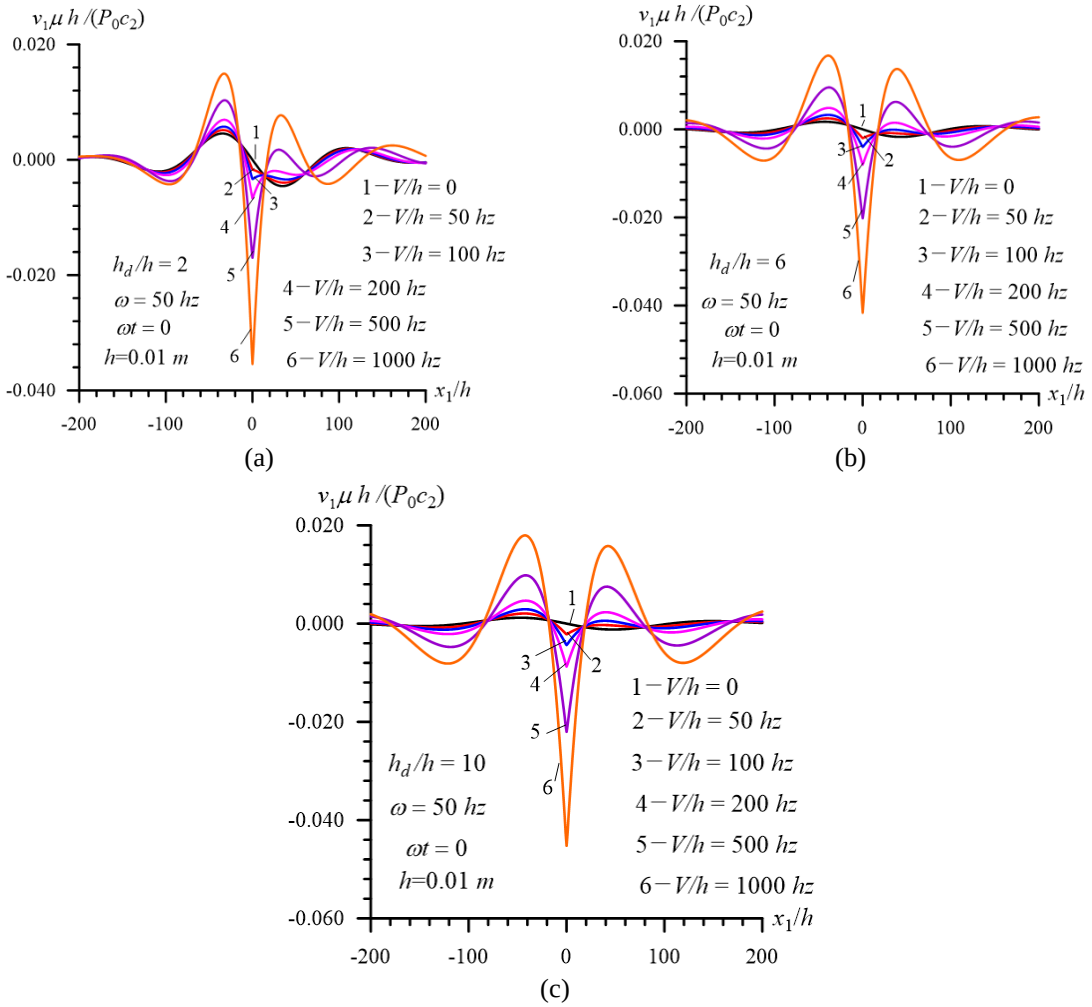

Fig. 13 The influence of the moving velocity of the oscillation load on the distribution of the velocity $v_1\mu h/(P_0c_2)$ under ωt=0 in the cases where h_d/h=2 (a), 6 (b) and 10 (c)

viscosity on the influence of the motion of the oscillation load on the distribution of the stress (on the distribution of the velocity) has a mainly quantitative character in the case where ωt=0 (in the case where ωt=π/2). At the same time, it follows from the results given in Fig. 14(b) (Fig. 15(a)) and from comparison of these results with those given in Fig. 11(b) (in Fig. 12(a)) that the effect of the fluid viscosity on the influence of the motion of the oscillation load is significant not only in the quantitative sense, but also in the qualitative sense. Note that the stress and velocity given in Figs. 14(b) and 15(a), respectively in the inviscid fluid case appear only as a result of the load moving, and their absolute values increase with this motion. Moreover, note that in the inviscid fluid case, the distribution of the stress under ωt=π/2 and the distribution of the velocity under ωt=0 are exactly asymmetric with respect to x_1/h=0.

Now, we consider the results illustrating how the moving of the oscillating load acts on the dependence between the studied quantities and vibration phase ωt. Graphs of this dependence are

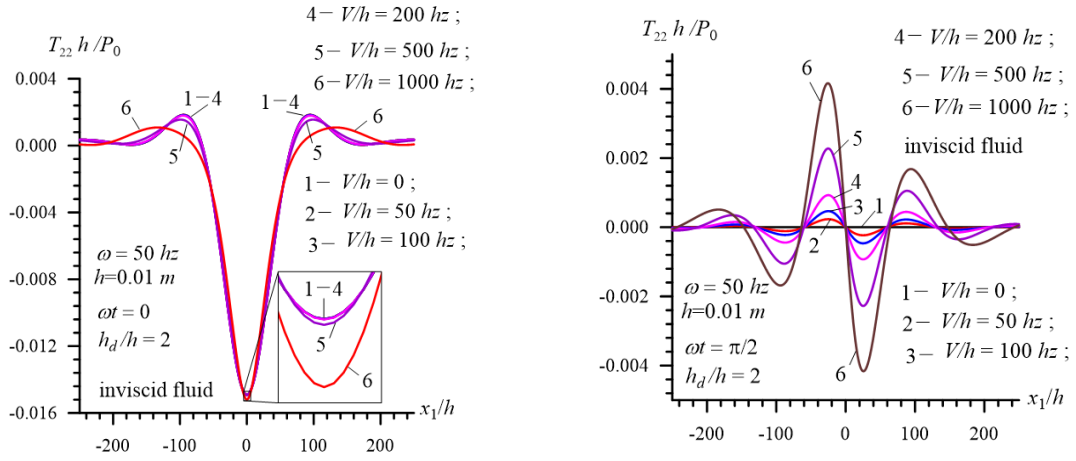

Fig. 14 Distribution of the stress $T_{22}h/P_0$ with respect to x_1/h under ωt=0 for various values of the moving velocity of the oscillation load in the inviscid fluid case

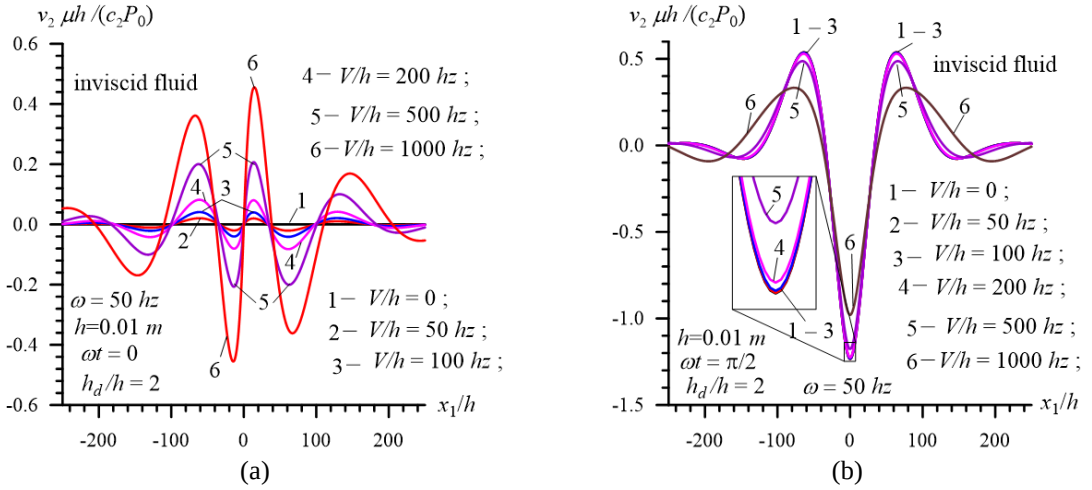

Fig. 15 Distribution of the velocity $v_2\mu h/(P_0c_2)$ with respect to x_1/h under ωt=0 for various values of the moving velocity of the oscillation load in the inviscid fluid case

given in Figs. 16, 17 and 18 for the stress $T_{22}h/P_0$, and velocities $v_2\mu h/(P_0c_2)$ and $v_1\mu h/(P_0c_2)$ respectively. Under construction of these graphs it is assumed that ω=50 hz and h_d/h=2, and various values of the load motion velocity are examined. In these figures, the graphs grouped by the letter a (by the letter b) relate to the case where the values of the studied quantities are calculated at point x_1/h=0 (at point x_1/h=−20). Thus, it follows from Fig. 16 that the influence of the moving velocity of the oscillating load on the dependence of the stress on the vibration phase at point x_1/h=0 is insignificant, but it is significant at point x_1/h=−20. At the same time, the character of this dependence at the points under consideration, is the same. Moreover, Figs. 17 and 18 show that the influence of the motion velocity of the oscillating load on the dependence between the velocities and vibration phase is significant not only at the point x_1/h=−20, but also at

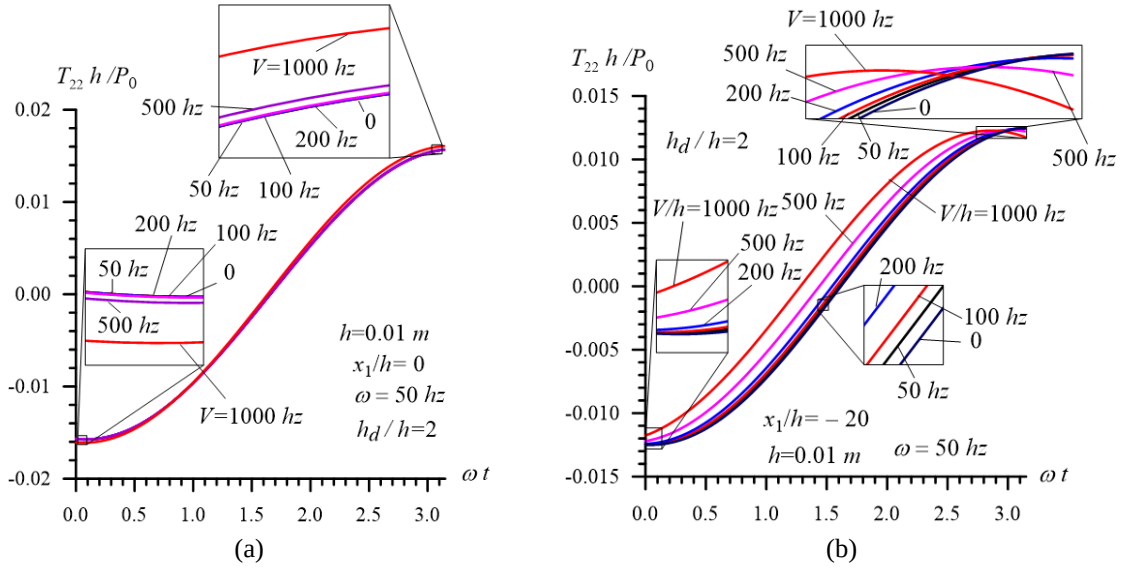

Fig. 16 Graphs of the dependence between the $T_{22}h/P_0$ and vibration phase ωt obtained for various values of the moving velocity of the oscillation load in the cases where x_1/h=0 (a) and x_1/h=−20 (b)

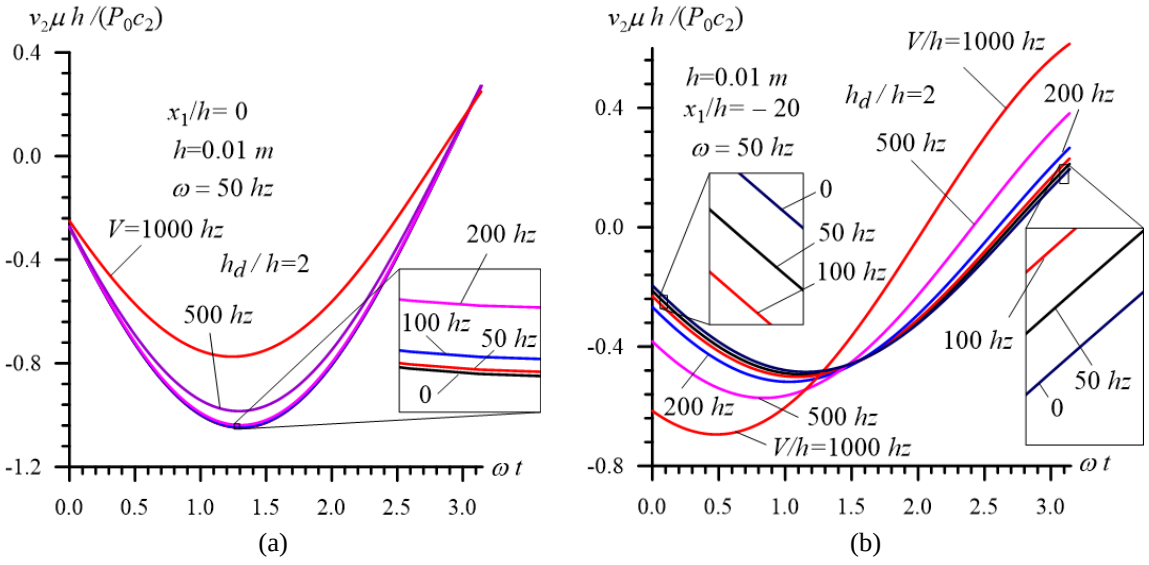

Fig. 17 Graphs indicated in Fig. 16 and constructed for the velocity $v_2\mu h/(P_0c_2)$

the point x_1/h=0. However, the character of this dependence obtained at point x_1/h=0 is different from that obtained at point x_1/h=−20. Consequently, we can conclude that the influence of the motion velocity of the oscillating load on the change of the studied quantities with respect to the vibration phase depends on the position of the point at which these quantities are calculated.

This completes the consideration of the numerical results.

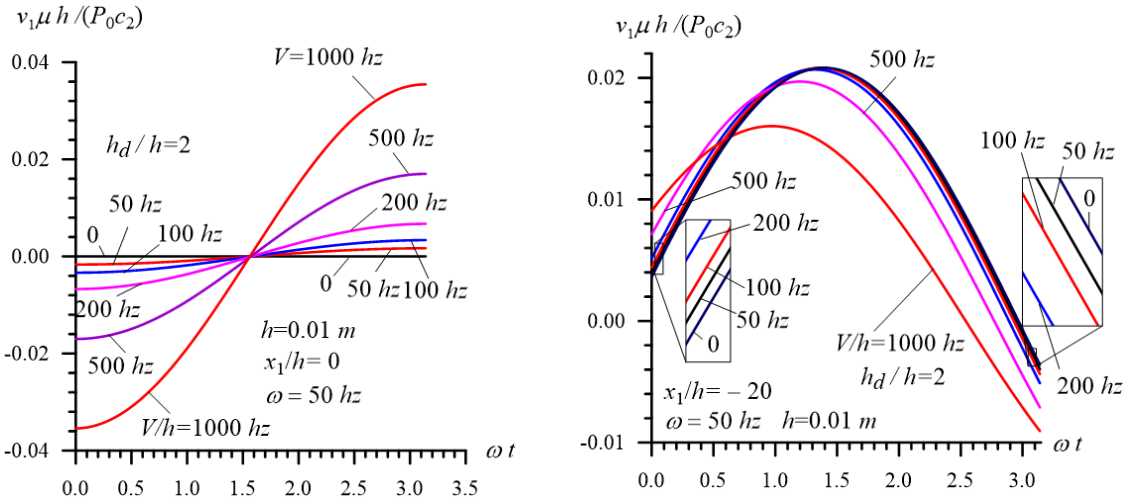

Fig. 18 Graphs indicated in Fig. 17 and constructed for the velocity $v_1\mu h/(P_0c_2)$

5. Conclusions

Thus, in the present paper the dynamics of the oscillating moving load acting on the hydro-elastic system consisting of the elastic plate, compressible viscous fluid and rigid wall has been studied.

The plane strain state in the plate is considered and the motion of the plate is described by utilizing the exact equations of elastodynamics. The corresponding plane-parallel flow of the fluid is described through the linearized Navier-Stokes equations. It is assumed that there is continuity of the force and velocity vectors of the constituents on the interface plane between the fluid and plate as well as impermeability conditions on the rigid wall. The corresponding boundary value problem is solved by employing the moving coordinate system and the exponential Fourier transformation with respect to the coordinate along the direction in which the plate lies. Originals of the sought values are determined numerically with the use of the algorithm and PC programs composed by the authors. Numerical results on the distribution of the stress and velocities with respect to the point of the interface plane are presented and discussed. According to these results and discussions, the following concrete conclusions can be drawn:

- The influence of the motion of the oscillating load on the distribution of the stress and velocities depends on the vibration phase of the system;
- In the vibration phases in which the studied quantities have their absolute maximum (denote it as “maximum” phase) under the corresponding time-harmonic load without moving, the influence of the moving of the oscillation load on the aforementioned distributions is insignificant;
- In the vibration phases in which the studied quantities have their absolute minimum (denote it as “minimum” phase) under the corresponding time-harmonic load without moving, the influence of the moving of the oscillating load on the aforementioned distribution is significant not only in the quantitative sense, but also in the qualitative sense;
- Under “maximum” phases, an increase in the values of the moving velocity of the oscillation

load causes an increase (a decrease) of the absolute maximum values of the stress (the velocities);

- Under "minimum" phases, an increase in the values of the moving velocity of the oscillating load causes an increase of the absolute maximum values not only of the stress, but also of the velocities;
- The motion of the oscillating load violates the symmetry and asymmetry of the studied quantities with respect to the loaded point which occurs under the corresponding time-harmonic loading without motion and this violation becomes more considerable in the "minimum" phases; and
- The influence of the motion velocity of the oscillating load on the change of the studied quantities with respect to the vibration phase depends on the position of the point at which these quantities are calculated.

References

Akbarov, S.D. (2015), *Dynamics of Pre-Strained Bi-Material Elastic Systems: Linearized Three-Dimensional Approach*, Springer, Heideiberg, New-York, Dordrecht, London.

Akbarov, S.D. and Ilhan, N. (2009), "Dynamics of a system comprising an orthotropic layer and orthotropic half-plane under the action of an oscillating moving load", *Int. J. Solid. Struct.*, **46**(21), 3873-3881.

Akbarov, S.D. and Ismailov, M.I. (2014), "Forced vibration of a system consisting of a pre- strained highly elastic plate under compressible viscous fluid loading", *CMES: Comput. Model. Eng. Sci.*, **97**(4), 359-390.

Akbarov, S.D. and Ismailov, M.I. (2015a), **"**The forced vibration of the system consisting of an elastic plate, compressible viscous fluid and rigid wall", *J. Vib. Control*, DOI: 10.1177/1077546315601299

Akbarov, S.D. and Ismailov, M.I. (2015b), "Dynamics of the moving load acting on the hydro-elastic system consisting of the elastic plate, compressible viscous fluid and rigid wall", *CMC: Comput. Mater. Continua*, **45**(2), 75-10.

Akbarov, S.D. and Salmanova, K.A. (2009), "On the dynamics of a finite pre-strained bi-layered slab resting on a rigid foundation under the action of an oscillating moving load", *J. Sound Vib.*, **327**(3-5), 454-472

Akbarov, S.D., Ilhan, N. and Temugan, A. (2015), "3D dynamics of a system comprising a pre-stressed covering layer and a pre-stressed half-space under the action of an oscillating moving point-located load", *Appl. Math. Model.*, **39**, 1-18.

Bagno, A.M. (2015), "The dispersion spectrum of wave process in a system consisting of an ideal fluid layer and a compressible elastic layer", *Int. Appl. Mech.*, **51**(6), 52-60.

Bagno, A.M. and Guz, A.N. (1997), "Elastic waves in prestressed bodies interacting with fluid (Survey)", *Int. Appl. Mech.*, **33**(6), 435-465.

Bagno, A.M., Guz, A.N. and Shchuruk, G.I. (1994), "Influence of fluid viscosity on waves in an initially deformed compressible elastic layer interacting with a fluid medium", *Int. Appl. Mech.*, **30**(9), 643-649.

Charman, C.J. and Sorokin, S.V. (2005), "The forced vibration of an elastic plate under significant fluid loading", *J. Sound Vib.*, **281**, 719-741.

Fu, S., Cui, W., Chen, X. and Wang, C. (2005), "Hydroelastic analysis of a nonlinearity connected floating bridge subjected to moving loads", *Marine Struct.*, **18**, 85-107.

Fu, Y. and Price, W. (1987), "Interactions between a partially or totally immersed vibrating cantilever plate and surrounding fluid", *J. Sound Vib.*, **118**(3), 495-513.

Guz, A.N. (2009), *Dynamics of Compressible Viscous Fluid*, Cambridge Scientific Publishers, Cottenham.

Guz, A.N. and Makhort, F.G. (2000), "The physical fundamentals of the ultrasonic nondestructive stress analysis of solids", *Int. Appl. Mech.*, 3**6**, 1119-1148.

Ilhan, N. and Koç, N. (2015), "Influence of polled direction on the stress distribution in piezoelectric materials", *Struct. Eng. Mech.*, **54**, 955-971.

Kwak, H. and Kim, K. (1991), "Axisymmetric vibration of circular plates in contact with water", *J. Sound Vib.*, **146**, 381-216.
Kwak, M.K. (1997), "Hydroelastic vibration of circular plates (Fourier-Bessel series approach)", *J. Sound Vib.*, **201**, 293-303.
Kwak, M.K. and Han, S.B. (2000), "Effect of fluid depth on the hydroelastic vibration of free-edge circular plate", *J. Sound Vib.*, **230**, 171-125.
Lamb, H. (1921), "Axisymmetric vibration of circular plates in contact with water", *Proceeding of the Royal Society (London) A*, **98**, 205-216.
Sorokin, S.V. and Chubinskij, A.V. (2008), "On the role of fluid viscosity in wave propagation in elastic plates under heavy fluid loading", *J. Sound Vib.*, **311**, 1020-1038.
Tubaldi, E. and Armabili, M. (2013), "Vibrations and stability of a periodically supported rectangular plate immersed in axial flow", *J. Fluid. Struct.*, **39**, 391-407.
Wang, C., Fu, S. and Cui, W. (2009), "Hydroelasticity based fatigue assessment of the connector for a ribbon bridge subjected to a moving load", *Marine Struct.*, **22**, 246-260
Wu, J.S. and Shih, P.Y. (1998), "Moving-load-induced vibrations of a moored floating bridge", *Comput. Struct.*, **66**(4), 435-461
Zhao, J. and Yu, S. (2012), "Effect of residual stress on the hydro-elastic vibration on circular diaphragm", *World J. Mech.*, **2**, 361-368.

CC